

CONF-850764--3

UCRL-92971  
PREPRINT

MOLECULAR DYNAMICS SIMULATIONS

B. J. Alder  
Lawrence Livermore National Laboratory  
University of California  
Livermore, CA 94550

This paper was prepared for submittal to  
Proceedings of the  
International School of Physics  
« Enrico Fermi »  
July 23 - August 2, 1985  
Varenna, Italy

July 1985



Lawrence  
Livermore  
National  
Laboratory

This is a preprint of a paper intended for publication in a journal or proceedings. Since changes may be made before publication, this preprint is made available with the understanding that it will not be cited or reproduced without the permission of the author.

B. J. Alder  
Lawrence Livermore National Laboratory  
University of California  
Livermore, CA 94550

UCRL--92971

DE85 015541

The molecular dynamics computer simulation discovery of the slow decay of the velocity autocorrelation function in fluids is briefly reviewed in order to contrast that long time tail with those observed for the stress autocorrelation function in fluids and the velocity autocorrelation function in the Lorentz gas. For a non-localized particle in the Lorentz gas it is made plausible that even if it behaved quantum mechanically its long time tail would be the same as the classical one. The generalization of Fick's law for diffusion for the Lorentz gas, necessary to avoid divergences due to the slow decay of correlations, is presented. For fluids, that generalization has not yet been established, but the region of validity of generalized hydrodynamics is discussed.

#### DISCLAIMER

This report was prepared as an account of work sponsored by an agency of the United States Government. Neither the United States Government nor any agency thereof, nor any of their employees, makes any warranty, express or implied, or assumes any legal liability or responsibility for the accuracy, completeness, or usefulness of any information, apparatus, product, or process disclosed, or represents that its use would not infringe privately owned rights. Reference herein to any specific commercial product, process, or service by trade name, trademark, manufacturer, or otherwise does not necessarily constitute or imply its endorsement, recommendation, or favoring by the United States Government or any agency thereof. The views and opinions of authors expressed herein do not necessarily state or reflect those of the United States Government or any agency thereof.

## 1. INTRODUCTION

The single most important fundamental discovery for the dynamic properties of interacting particles by computer simulation is that the molecular chaos approximation is generally not valid. In fact, the molecular chaos approximation, which implies that a particle after a sufficiently long time forgets its past, or equivalently, that correlations decay exponentially, is not valid for even the simplest models, such as a dilute gas or a Lorentz gas. This approximation was originally introduced because it seemed physically reasonable and because it led to a great mathematical simplification, namely that, dynamic processes could be described by Markov processes. By computer simulation, before real experiments such as neutron diffraction studies, it was possible to investigate the decay of correlations with sufficient resolution to show that the decay had a long time tail, corresponding to a power law fall-off with time [1]. This discovery caused a fundamental change in the mathematical structure with which to describe transport properties. For example, the Boltzmann equation and the Chapman-Enskog expansion used in its solution can be shown not to be valid for a finite density gas. This discovery, however, also initiated a stampede that ascribed all tails that have been subsequently discovered to the same mechanism. The primary focus of this report is to demonstrate the differences between various tails.

For that purpose, the tails of the Lorentz gas will be discussed since that is the simplest model for which such tails might be analyzed, because only the motion of a single point particle among randomly arranged fixed scatterers is involved. In order to contrast the tails of the Lorentz gas with that of others that occur in fluids, however, a brief review of their characteristics will be given. At least one of these other tails, that for the diffusion coefficient of fluids, is due to collective phenomena; that is,

due to the cooperative motion of the particles in the medium, which by the very nature of the Lorentz model cannot occur in that system. The nature of the collective mode in the diffusion case can be identified with great confidence since a hydrodynamic model confirmed by molecular dynamic results yielded quantitative agreement [2]. The only other important collective effect that was discovered by molecular dynamics in fluid transport phenomena was in the slow decay of the stress autocorrelation function that determines the viscosity [3]. That tail, called the molasses tail to distinguish it from the hydrodynamic tail for diffusion, has also been analyzed by the same methods as for diffusion with far from quantitative success. As shall be seen, the employment of a hydrodynamic type analysis for all tails including that for the Lorentz gas is of doubtful validity.

## 2. HYDRODYNAMIC TAIL

The decay of the velocity autocorrelation function,

$$(2.1) \quad \rho(t) = \langle v(0)v(t) \rangle / \langle v^2(0) \rangle$$

at intermediate fluid densities is illustrated in Fig. 1a. The velocity autocorrelation function, whose integral is the diffusion coefficient, shows a positive persistence of velocity that can be observed for some 100 collisions. That positive tail can be quantitatively accounted for by a hydrodynamic model in which a sphere, surrounded by a continuum fluid, characterized by a compressibility and a viscosity, is given an initial velocity or momentum [1]. Those initial conditions lead to a positive pressure in the fluid ahead of the sphere that generates a sound wave and a

corresponding rarefaction wave behind. In addition, the positive pressure in front and the negative pressure behind can equalize by creating a double vortex structure around the sphere. This phenomena is vividly verified by investigating the velocity field =  $\sum_{j=1}^n V_i(0) V_j(t)$  surrounding the sphere, by molecular dynamics [2]. The velocity field is the correlation between the original velocity of the sphere,  $i$ , and the net velocity of all the particles,  $j$ , in a surrounding volume element at some time,  $t$ , later. The agreement between this molecular dynamically determined velocity field and the corresponding hydrodynamic one is quantitative after some 10 collisions, or about  $10^{-13}$  sec. The remarkable validity of hydrodynamics at this time scale and distance scale of only a few molecular diameters will be referred to again later. A dimensional analysis of the hydrodynamic model leads to a quantitative description of the tail. After first observing that at long times only the vortex mode contributes since it spreads diffusively as the square root of  $\nu t$  while the sound wave spreads faster, namely to further distances as  $ct$ , where  $\nu$  is the kinematic viscosity, (the shear viscosity divided by the density) and  $c$  is the speed of sound. Since momentum, (mass times velocity =  $mv$ ) is conserved,  $m \int v d\tau$  must be a constant, where  $\tau$  is the volume element, which must be integrated over the entire space to account for all the momentum. Since  $\tau$  spreads as  $(\nu t)^{d/2}$ , where  $d$  is the dimensionality of the space,  $v$  must decay as  $(\nu t)^{-d/2}$  to keep the momentum constant. The more difficult but readily doable task is to determine the coefficient  $A$  in the power law decay of the velocity,  $A/(\nu t)^{d/2}$ , since that requires knowing how much of the momentum is carried away by the sound wave and how much of the rest is fed back via the medium to the moving sphere. This same power law has also been derived by graph theoretical methods involving summation of ring diagrams [4] that have intuitively close

correspondence to vortex rings. Other derivations by mode coupling theories [5] also have their origin in hydrodynamic arguments. Finally, a derivation by renormalization theory has also been carried out. Not surprisingly, renormalization theory applies since the exponent is universal, namely, it does not depend on any of the detailed molecular properties of the system.

### 3. MOLASSES TAIL

The velocity autocorrelation function at higher density, near normal liquid density, is shown in Fig. 1b. In that case, the positive tail has not been observed because it is overpowered by a negative feature in the velocity autocorrelation function near solid densities caused by a reversal of the velocity of a typical particle by backscattering. This effect can only be accounted for hydrodynamically by introducing viscoelastic effects, as shall be seen later. These significant viscoelastic effects are a reflection of the slow decay of the stress autocorrelation function, shown in Fig. 1c., dubbed the molasses tail. For the molasses tail, the hydrodynamic, or graph theoretical analysis [6], again leads to a tail of the form  $A'/t^{d/2}$ , but the molecular dynamics results have only established the appropriateness of the power law over a very limited time domain and with a value of  $A'$  which is at least an order of magnitude larger than the theoretically predicted one [7]. We believe that this theoretical prediction is appropriate only for the kinetic part of the viscosity. A considerable effort to observe this tail for the kinetic part of the viscosity failed, however, because the numerical resolution was not high enough [8].

An investigation as to the origin of the molasses tail is underway. Just as the diffusion coefficient can be calculated by  $D = \langle \Delta X^2 \rangle / 2t =$

$\int_0^{\infty} \langle \dot{X}(0)\dot{X}(t) \rangle dt$ , so can the viscosity from  $\eta = \langle \Delta G^2 \rangle / 2t = \int_0^{\infty} \langle \dot{G}(0)\dot{G}(t) \rangle dt$ , where  $G$  is the dynamic variable  $G = \sum_i x_i \dot{y}_i$  and  $\Delta G = \int_0^t \dot{G} dt$ , the potential part of which is  $\sum_{ij} x_{ij} \dot{\Delta y}_{ij}$ , where the dot indicates differentiation with respect to time and the subscripts  $ij$  indicate that the two hard sphere particles  $i$  and  $j$  are in collision. Upon differentiating  $G$ , two terms arise. The first one involves  $\dot{x}\dot{y}$  and leads to the kinetic term discussed above, whose tail was found to be unobservable. The second, or potential term, involves  $x\ddot{y}$  or  $xV'$ , where the acceleration has been replaced by the force, or derivative of the potential. It is that term that develops the molasses tail but only near solidification densities. It appears to be connected with a slow structural adjustment in the presence of a shear. A likely mechanism for this structural rearrangement is a slight ordering or layering of the spheres parallel to the plane of the shear so as to reduce the resistance to flow. It is analogous to the ordering of asymmetric molecules in the presence of a velocity gradient in such a way that the long axis is preferentially parallel to the flow. For spherical particles, many structural effects have been observed for colloidal suspension in fluids and by nonequilibrium molecular dynamics calculations in the presence of an enormous, externally imposed, shear [9]. For these spherical particles the manifestations are a decrease in the viscosity with shear rate, called shear thinning, which, with sufficiently high shear rate, dramatically results in shear induced ordering or solidification.

The likely cause for the slowness of the response is that this partial ordering process involves, at high density, a large number of particles, namely all those within the correlation length (the distance beyond which the radial distribution function becomes constant). The long correlation is not likely to be between successive magnitudes of the velocity changes upon collision,

$|\Delta\dot{y}_{ij}|$ , in the expression for  $\langle \Delta G^2 \rangle$  since the absolute value of velocities were found to equilibrate fast even at high density. The hypothesis that is being tested is that successive angles between collisions are correlated. Formally, that means one would like to show that at long times the auto-correlation of  $\sum x_{ij}y_{ij}$  and of  $\sum x_{ij}\dot{y}_{ij}$  for colliding particles have the same behavior. Certainly,  $\sum x_{ij}y_{ij}$  will have an infinitely ranged correlation in the solid phase in as much as the angle between any pair of successive collisions will stay fixed on the average even if the pairs are separated by very large distances. This is then consistent with the known infinite viscosity in the solid phase. Furthermore, such slow decay of correlations have been observed already in a very similar autocorrelation function, namely the one for dipolar density fluctuation  $\sum_{i<j} x_{ij}y_{ij}/r_{ij}^5$  appropriate to depolarized light scattering calculations [10], where the sum is now over all pairs in the system, not just those in collision. In fact, that autocorrelation was observed to decay even slower than that of the stress which can be explained by noting that the dipole autocorrelation function is more long ranged. In the dipolar case, the calculation was broken down into its three components corresponding to correlations between the same pair of particles, two different pairs sharing one particle in common, and two totally different pairs. A similar breakdown in the stress case would help identify the contributor to the slow decay.

Hopefully, these studies will ultimately lead to a model for the molasses tail, but it is unlikely to be of simple hydrodynamic origin. Such a model is of particular interest in the theory of glass formation. A proper dynamical theory of the glass transition identifies the stable amorphous state as the point at which the viscosity becomes infinite along the metastable fluid branch [11]. However, to predict the cooling rate necessary to prevent



crystallization requires knowledge of the rate of growth of the molasses tail for a cluster the size of a critical solid nucleus compared to the rate of formation of that critical sized nucleus. That is, one needs to know the rate of decay of the molasses tail for the viscosity at the appropriate wave vector so that it can be compared to the rate at which the system tries to crystallize.

#### 4. LORENTZ TAILS

The tails in the Lorentz gas are of a still different nature than the ones discussed so far. They are illustrated in Fig. 1d and are characterized by a slow decay in the negative region of the velocity autocorrelation function and can be observed at all densities of the random scatterers, even when the diffusion coefficient vanishes, and for all sorts of different types and arrangements of the scatterers. We shall confine our discussion to two dimensional systems since these are the most interesting in the sense that sometimes they behave like one-dimensional systems that have zero diffusion coefficients even in the low density limit and sometimes they imitate three dimensional systems with vanishing diffusion coefficients only at high density, above a percolation density. The class in which the tails fall depends on the restriction on the degree of freedom of motion that is imposed on the model. We shall also confine our discussion primarily to hard square and hard disk scatterers in various random arrangements such as overlapping and non-overlapping. For squares we shall also consider various random arrangements of the squares on a chess board and, furthermore, not only impenetrable squares. The latter is of interest as a model for scattering of electrons in a two dimensional metallic fluid as proposed by Anderson, and

hence we also discuss the quantum mechanical version of the Lorentz gas. In the Anderson Model, the question again concerns whether or not it falls in the one dimensional class, that is, whether the resistance of a fluid metal film never vanishes.

The negative tails in the Ehrenfest wind tree model can be ascribed to the higher than random probability of return of the particle (the wind) to its point of origin [12]. The trees in that model are squares placed with their diagonals along either the x or y axis. The particles are also started off moving in only the x or y direction and because of the geometry will subsequently confine their motion to these two directions only. In the overlapping version of the Ehrenfest model it can then be shown by graph theoretical methods that the diffusion coefficient vanishes even in the low density limit with a power law tail whose exponent is a known function of density. The vanishing of the diffusion coefficient arises because sooner or later a particle will exactly collide at the intersection of two overlapping squares, where upon it must exactly retrace its path back to the origin. This graph theoretical prediction was confirmed by computer simulation [12]. This restricted motion model hence falls in the one dimensional class.

In the case of non-overlapping squares in the Ehrenfest model, the analysis yields a nonvanishing diffusion coefficient with a tail of the same type as in the overlapping case but with different constants in the functional density dependence. Also in the case of overlapping disks, the diffusion coefficient is finite below the percolation density, again with a tail of the same form with still different constants both above and below the percolation density. In all these cases, whether the particle is trapped or not, there are negative tails caused by the higher than random probability of return paths, but the power law that describes the tail is first of all not universal

since it depends on the density of the fixed random scatterers and secondly differs in detail in the constants depending on the shape of the objects that do the scattering on the intermolecular potential. This is to be contrasted with the hydrodynamic tail where a universal mechanism determines the power law with a power that depends only on the dimensionality.

The graph theoretical arguments so far have only been able to predict the power law constant in the disk case in the low density limit [12]. The mode coupling or hydrodynamic-like models predict that this low density power law constant holds universally at all densities and for all shapes of scatterers. This ignores the known difference in the constant between squares and disks even in the low density limit. Furthermore, this disagrees with computer simulation results which show a decided density dependence in the power law behavior at long enough times where the lack of a density dependence should have become apparent. It thus appears that the power law decay of the tail depends on the topological details and that hydrodynamic scaling or renormalization arguments can not be applied. Such arguments have also been used for the quantum Lorentz gas and the conclusions therefore are hence suspect.

Rigorous mathematical analysis of the disk Lorentz gas are, in fact, of topological origin, but so far, only very limited in scope. The only relevant proof is that in periodic space, the tail is exponential in character [14]. In periodic space you do not have random scatterers and, indeed, as Fig. 2 shows in the case of an ordered high density solid consisting of disks, the envelope of the oscillating velocity autocorrelation function is of exponential character. This is to be contrasted with the disordered non-overlapping disk solid where the velocity autocorrelation function after a few oscillations has a power law tail.

We now return to the question of when a diffusion constant exists. Rigorous arguments in favor of the existence of a diffusion constant have been made for the Lorentz gas but unfortunately only under the restriction of the Boltzmann-Grad limit [15]. In that limit, long retracing trajectories are eliminated by a finite free path cut off. Hence, this theorem cannot distinguish between the overlapping square and disk model. In the latter, because particles can move in all directions, the probability of exactly colliding at the intersection of two disks is much lower (zero measure) so that the diffusion coefficient exists, but nevertheless, the probability of returning is sufficiently high to produce a long tail. Thus, the disk case falls into the three dimensional class. There are variations of the square model that fall in between the Ehrenfest and disk case that are presently under investigation to determine in which category they belong. One such variation is randomly occupied squares on a chessboard where the particle can start off in any direction. A variation on that is that the randomly blocked squares can only be among the black squares of the chessboard, so that squares can only touch occasionally at their corners.

These square models are artificial. However, if scaling were to work, that would not matter. In the band theory of metals such square models are a natural extension to two dimensions of the repeated square-well square mound potential used in one dimensional versions. It can be shown in one dimension that if the potential is regular, that is the height and width of the square-wells and square-mounds are repeatedly the same, a metallic conduction band results. On the other hand, it can be shown that if the depth of the square-well and the height of the square-mound are randomly selected between bounds, then the diffusion coefficient vanishes and the particle is bound no matter what its energy is relative to the mound. Anderson has argued that the

two dimensional version of this, where the squares on a chessboard have random heights and depths between bounds, behaves as the one-dimensional model [16]. Although the proof in one dimension is rigorous, the one in two dimensions assumes the validity of scaling. It is just this scaling that has been questioned for classical Lorentz gases. We have therefore started to investigate two aspects of the Anderson model. The first one is the classical limit of that model to test whether it follows scaling and whether it conforms to the Anderson prediction of localization no matter what the energy of the particle is. The preliminary results are presented in fig. 3 and are negative on both counts. Given the Bohr correspondence principle one could still argue that Anderson might be right if the limit of Plank's constant going to zero is not approached uniformly. There are precedents for the limiting process and the limit being different, particularly for discontinuous potentials. In the classical limit of the Anderson model, three different regimes can be recognized. When the energy of the particle is less than half the maximum possible mound height or depth, the particle appears to be trapped, leading to an oscillating and rapidly decaying velocity autocorrelation function. If the energy of the particle is in between half and the maximum mound value, the particle diffuses with a long negative power law tail, while with an energy above the mound, the diffusion coefficient is enormous due to a positive power law tail. The power law of the tail appears to be energy dependent, thus making scaling inoperative.

The second aspect of the Anderson model investigated is its dynamical aspects. That is, we solved the time dependent Schrödinger equation for a particle propagating through a random arrangement of overlapping disks in order to confirm a conjecture; namely, that at long times such a quantum mechanical system has the same behavior as a classical system provided the

particle is not trapped. A loose argument in favor of this is that letting  $\hbar$  go to zero is equivalent to letting time go to infinity. A slightly more serious argument is to write the time dependent Schrödinger equation in terms of an amplitude  $A$  and a phase  $S$ , that is

$$(4.1) \quad i\hbar \frac{\partial \phi}{\partial t} = -\hbar^2/2m \nabla^2 \phi + V\phi$$

$$\text{and} \quad \phi = Ae^{iS/\hbar}$$

so that under this Madelung transformation

$$(4.2) \quad \frac{\partial A}{\partial t} + \vec{\nabla} \cdot (A^2 \vec{\nabla} S/m) = 0$$

$$(4.3) \quad \frac{\partial S}{\partial t} + \frac{(\vec{\nabla} S)^2}{2m} + V = \frac{\hbar^2}{2m} \frac{\nabla^2 A}{A}$$

If  $\hbar$  is set to zero in these two equations, we recognize that they reduce to the classical Hamilton-Jacobi equations if  $\vec{\nabla} S/m$  is interpreted as a velocity. The question then is under what circumstances does  $\nabla^2 A/A$  vanish, so that the condition under which a single particle quantum system behaves classically can be specified. If we make the reasonable assumption that the probability distribution,  $\psi^* \psi = A^2$  is Gaussian at long times, that is  $\psi^* \psi = c \exp(-x^2/\langle x^2 \rangle)$ , with a half width  $\langle x^2 \rangle = \int \psi^* x^2 \psi dJ = Bt^\alpha$  which has a long time tail with a positive power  $\alpha$ , then  $\nabla^2 A/A = -1/Bt^\alpha$ . Thus the  $\nabla^2 A/A$  term vanishes in the long time limit unless  $\alpha = 0$ , in which case the particle is trapped since  $\langle x^2 \rangle$  is bounded. Note that even if  $\alpha$  is between zero and unity and hence the diffusion coefficient  $\langle x^2 \rangle/t$  vanishes, the conjecture still holds because the wave function is still spreading.

The weakest point in the above argument is that  $\psi^* \psi$  is a smooth Gaussian. For any individual experiment the wave function is locally not smooth, for example near a scatterer. However, for an ensemble average, the assumption is likely to be valid. Thus we have committed the crime of interchanging differentiation and ensemble averages, but we are in good company. Since as fluctuation theory only holds for an average velocity autocorrelation function, any individual velocity changes upon collisions can be enormous. We thus believe that the tail in the quantum and classical velocity autocorrelation functions have the same power law. The numerical evidence given in Fig. 4 is as yet too crude to say this with confidence. If it proves to be correct, an enormous amount of computer time could be saved in the investigation of tails in the quantum case, since the equivalent classical systems run orders of magnitude faster.

There are two more points to be made with respect to quantum calculations. One is that in the following paper we present another conjecture that would be very useful in chemical rate calculations; namely, that in steady state calculations, the long time behavior of the probability density is the same in real and imaginary time calculations. The latter are very much easier to implement. The other point is that very convincing numerical quantum mechanical calculations have been made that confirm Anderson's localization prediction in two dimensions [17]. The criticism that can be leveled at these calculations is that they are quasi-one-dimensional, because in the narrow strips they investigated, the correlation length near a possible critical point exceeded the width of the system. A proper extrapolation to large two dimensional systems requires that in that process the width to correlation length ratio be kept constant.

## 5. GENERALIZED HYDRODYNAMICS

One of the consequences of the long time tails is that none of the Taylor series expansions of the transport coefficients, such as in density, temperature, wavelength, frequency, gradients, etc. exist. As an illustration of the divergences, the linear Burnett coefficients for diffusion for the Lorentz gas will be discussed, because this is the only case for which the expansion could be re-expressed so that it is convergent. The reason for the divergences is that, because of the long time memories which the tail represents, the distribution of distances a particle travels in a given time is not Gaussian except in the infinite time limit. In that limit, the second moment of that Gaussian, or the half width, determines the diffusion coefficient. However, the next moment or cumulant, which is the first Burnett coefficient,  $[\langle \Delta x^4 \rangle - 3 \langle \Delta x^2 \rangle^2]/t$ , exists only if the distribution approaches the Gaussian as a Gaussian, which, because of the long memory effects, is not the case [18]. Another way to see the divergence is to utilize the dimensional arguments by which the tail for the diffusion coefficient was analyzed. If  $\langle \Delta x^2 \rangle/t$  had a tail of  $t^{-\alpha}$ , then  $\langle \Delta x^4 \rangle/t$  must have a tail one power of  $t$  higher, namely  $t^{-\alpha+1}$ . Indeed, the computer results for the Lorentz gas confirmed that each successive Burnett coefficient has a tail one power of  $t$  higher than the previous one and thus sooner or later the higher ones will diverge.

The Burnett coefficients measure the dependence of the transport coefficients on the size of the relevant gradient, that is, on the wavelength of the fluctuation. The Burnett coefficients are also the coefficients that appear in the Chapman-Enskog expansion for the Boltzmann equation and in the higher order corrections to Fick's law for diffusion



$$(5.1) \quad \frac{\partial f(x,t)}{\partial t} = D \frac{\partial^2 f}{\partial x^2} + B \frac{\partial^4 f}{\partial x^4} + \dots$$

where  $f$  is the distribution function, and  $B$  the first linear Burnett coefficient. The proper generalization of Fick's law that leads to a redefinition of the Burnett coefficients which is well behaved is shown both by computer simulation [18] and graph theoretical analysis to be

$$(5.2) \quad \frac{\partial f(x,t)}{\partial t} = \int_0^t \rho(t-t') \frac{\partial^2 f}{\partial x^2} dt' + \frac{B}{D} \int_0^t \rho(t-t') \frac{\partial^4 f}{\partial x^4} dt' + \dots$$

If the velocity autocorrelation function,  $\rho$ , is short ranged, then the expression reduces to the older theory. If that is not the case, a non-local in time memory function that is both non-local in time as well as sparse must be introduced to obtain a convergent series. That memory function has not been firmly established. In the Lorentz gas with stationary scatterers such non-local spatial correlations can not develop. Another simplification in the Lorentz gas is that all the higher Burnett coefficients have the same memory function, which may not be the case in fluids. For the non-linear Burnett coefficients, namely coefficients of the form of  $\left(\frac{\partial^2 f}{\partial x^2}\right)^2$ , even the appropriate fluctuation dissipation expression of the Kubo form has not yet been formulated, although it too is expected to diverge.

Even though the dependence of the generalized transport coefficients on the wavelength, the frequency, and the amplitude of the fluctuation is not analytic, there exists fluctuating hydrodynamic formulations for these generalized coefficients that are amenable to calculation by molecular dynamics [19] and which determine the value of the transport coefficients for specific values of the wavelength and the frequency, but, as mentioned above, this is not the case for the amplitude. The latter formulation is being

worked on, and thus we can only discuss generalized linear transport theory. The purpose of generating these generalized linear transport coefficients is to replace the constant transport coefficients in the Navier-Stokes equations by them so as to introduce a length and time scale into the hydrodynamic equations. From that it is possible to learn to what small distance and short time scales hydrodynamics can be pushed. We already know from the hydrodynamic model for the tail that hydrodynamics applies on a submicroscale and at less than picosecond times. We also know that in order to explain the negative feature in the velocity autocorrelation function near solidification densities by a hydrodynamic model a non-local wavelength and frequency dependent viscosity is required. The primary cause of this non-locality in time of the viscosity is the molasses tail. We furthermore know that such a viscosity is required to explain shear mode propagation observed in the fluid phase near solidification in the neutron scattering function.

The only hydrodynamic problem actually solved so far with generalized transport coefficients is the Stokes problem of an infinitely massed sphere falling in a fluid, in order to find out what the corrections to Stokes law would be if the sphere was of atomic dimensions [19]. Indeed, it was found that the corrections were small, only about 30% for the friction coefficient compared to the macroscopic sized sphere. In general, it is extremely difficult to solve the Navier-Stokes equation with non-local transport coefficients. It is hard enough to solve the ordinary Navier-Stokes equation with constant coefficients even when the non-linear (in the square of the velocity) term that leads to hydrodynamic instabilities such as turbulence is left out. Usually, further simplifications such as incompressibility or inviscidness have to be introduced to simplify the mathematics. Yet, frequently the physical situation is even more complex, particularly in those

leading to hydrodynamic instabilities. Then, the fluid often contains regions where the gradients are steep. However, even the equations to describe that situation are not yet formulated, let alone numerically tractable.

There now emerges a possibility to circumvent, at least for some physical situations, this complex program of calculating the linear and non-linear generalized transport coefficients and introducing them into the conservation laws, leading to Navier-Stokes type of equations that are computationally difficult to solve. That scheme takes advantage of the earlier observations that hydrodynamics works on an atomic scale; namely, it suggests to simulate via molecular dynamics directly the hydrodynamic problem. Thus, instead of solving the Navier-Stokes equations, solve the Liouville equation for perhaps 100,000 particles for initial conditions which mock up the physical situation. Encouraging results in that direction have recently been obtained for a plate representing a satellite entering the earth's atmosphere near sound speed velocities [20]. Using 40,000 particles to represent the three dimensional medium allowed the system to be some one hundred mean free paths wide. The solid plate width was a substantial fraction of the width of the system. The velocity field and streamlines that were calculated by molecular dynamics showed clear evidence of the alternate vortex shedding phenomenon leading to realistically working wakes behind the plate. The comparable hydrodynamic problem has yet to be solved. It appears that as computers can handle bigger and bigger molecular dynamic systems for longer and longer times, the direct simulation of complex hydrodynamic phenomena is a practical possibility. In the above problem it would have been possible to represent the plate and hence the solid-fluid boundary conditions more realistically by having the solid plate made up of particles as well. What may ultimately be most effective is to solve the hydrodynamic problem on a molecular scale until

the non-linear and memory effects have disappeared and then feed that molecular dynamic solution as an input to the Navier-Stokes equation to pursue the problem to macroscopic distance and time scales.

In this connection it is worthwhile to briefly summarize under what circumstances one needs to use what form of linearized, generalized hydrodynamics, and where one only needs ordinary hydrodynamics. That is, where ordinary ( $k = 0, \omega = 0$ ) transport coefficients suffice. For orientational purposes  $k\sigma = 2\pi$  or  $1/k\sigma \sim 0.15$  represents the atomic spacing and  $V/V_0 = 5$  corresponds roughly to the critical liquid-gas point volume of a fluid, while  $V/V_0 = 1.5$  is the fluid-solid coexistence volume. As can be seen from Fig. 5, ordinary hydrodynamics works beyond some 20 intermolecular spacings or some 100 Å at all densities. For smaller distances, the hydrodynamic relaxation time,  $(\nu k^2)^{-1}$ , is not long compared to the molasses tail relaxation time and viscoelastic effects appear and a time or frequency dependent viscosity needs to be used. At lower densities, however, where there is no significant molasses tail, such a region never appears nor does there appear a region where both non-locality in space and time has to be taken into account. However, when the wave number gets to be such that wavelengths less than an intermolecular spacing are considered, the continuum approximation of hydrodynamics starts to breakdown. On the other hand, kinetic theory becomes valid and hydrodynamics can be converted to kinetic theory by the device of using wavelength dependent transport coefficients. However, when the distances to be considered are smaller than a mean free path, the whole approach breaks down.

**ACKNOWLEDGEMENTS**

I want to thank Ed Alley and Scott Futral for their significant contributions to this paper. Work performed under the auspices of the U.S. Department of Energy by the Lawrence Livermore National Laboratory under contract number W-7405-ENG-48.

REFERENCES

- [1] B. J. Alder and T. E. Wainwright; Phys. Rev. A 1, 18 (1970).
- [2] B. J. Alder and T. E. Wainwright; J. Phys. Soc. Japan 26, 267 (1969).
- [3] B. J. Alder, D. M. Glass, and T. E. Wainwright; J. Chem. Phys. 53, 3813 (1970).
- [4] J. R. Dorfman and E. G. D. Cohen, Phys. Rev. Lett., 25, 1257 (1970).
- [5] H. H. H. Yaran and I. Oppenheim, Physica 90A, 561 (1978).
- [6] D. J. Evans, Nonlinear Fluid Behavior, editor H. J. M. Hanley, North Holland, Amsterdam 1983.
- [7] B. L. Holian and D. J. Evans, J. Chem. Phys. 78, 5147 (1983).
- [8] B. J. Alder, T. E. Wainwright, and D. M. Gass, Phys. Rev. A 4, 233 (1971).
- [9] J. Erpenbeck, Phys. Rev. Lett. 52, 1333 (1984).
- [10] B. J. Alder, H. L. Strauss, and J. J. Weis, J. Chem. Phys. 59, 1002 (1973).
- [11] E. Leutheusser, Phys. Rev. A 29, 2765,(1984).
- [12] E. H. Hauge and E. G. D. Cohen, J. Math Phys. 10, 379 (1969).
- [13] W. W. Wood and F. Lado, J. Chem. Phys. 7, 528 (1971).
- [14] L. A. Bunimovich and Y. Sniai, Com. Math Phys. 78, 479 (1981).
- [15] J. L. Lebovitz and H. Spoon, J. Stat. Phys. 19, 633 (1978).
- [16] E. Abrahams, P. W. Anderson, D. C. Licciandello, and T. V. Ramakvishman, Phys. Rev. Lett. 42, 673 (1979).
- [17] A. MacKinnen and B. Kramer, Phys. Rev. Lett. 49, 695 (1982).
- [18] B. J. Alder and W. E. Alley, Perspective in Statistical Physics, Ed. H. Ravechi', North Holland, Amsterdam 1981.
- [19] W. E. Alley and B. J. Alder, Phys. Rev. 27, 3158 (1983).
- [20] E. Meiburg, Phys. Fluids, to be published.

FIGURE CAPTIONS

Fig. 1 Schematic diagrams for different tails in 2 dimensions.

- (a) The velocity autocorrelation function for fluids at intermediate densities leading to a hydrodynamic tail.
- (b) The velocity autocorrelation function for fluids near solidification.
- (c) The stress autocorrelation function for fluids near solidification leading to a molasses tail.
- (d) The velocity autocorrelation function for the Lorentz gas with a geometry dependent tail.

Fig. 2 The velocity autocorrelation function for an ordered disk Lorentz gas contrasted with the one for a disordered non-overlapping solid at the same density,  $A/A_0 = 1.1$  where  $A_0$  is the area at close packing. The solid line is an empirical power law fit to the disordered case. The velocity autocorrelation function is normalized to unity at zero time and time is given in terms of collision times.

Fig. 3 Comparison for the classical version of the two dimensional Anderson model of the velocity autocorrelation function at three different energies relative to the maximum scattering potential,  $V_0$ . The solid lines represent the case for 1.1, the dotted line for 0.9, and the dashed line for 0.4.

Fig. 4 The mean square distance traveled for a quantum particle in the two dimensional Anderson model as a function of collision time in units of the disk radius,  $r$ , at a value of  $nr^2 = 0.24$  and an energy = 10 in  $\hbar/mr$  units, where  $n$  is the number density of scatterers. The slope at long times corresponds to the diffusion coefficient, which is comparable to the classical one.

Fig. 5 Schematic diagram denoting the various regimes of validity of different forms of generalized hydrodynamics for hard sphere fluids depending on the density,  $V/V_0$ , given as the volume,  $V$ , relative, to the close packed volume  $V_0$ , versus the reciprocal wave number,  $k$ , times the hard sphere diameter  $\sigma$ .



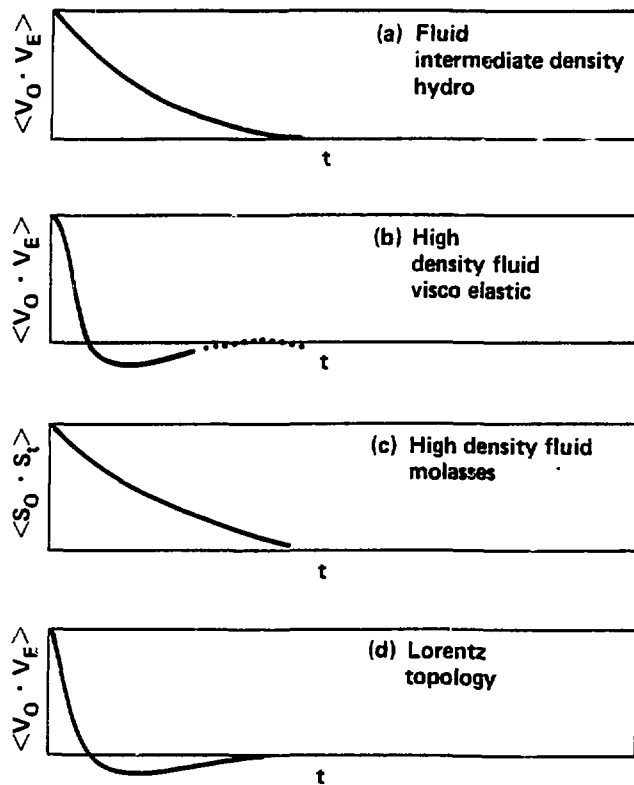


Figure 1

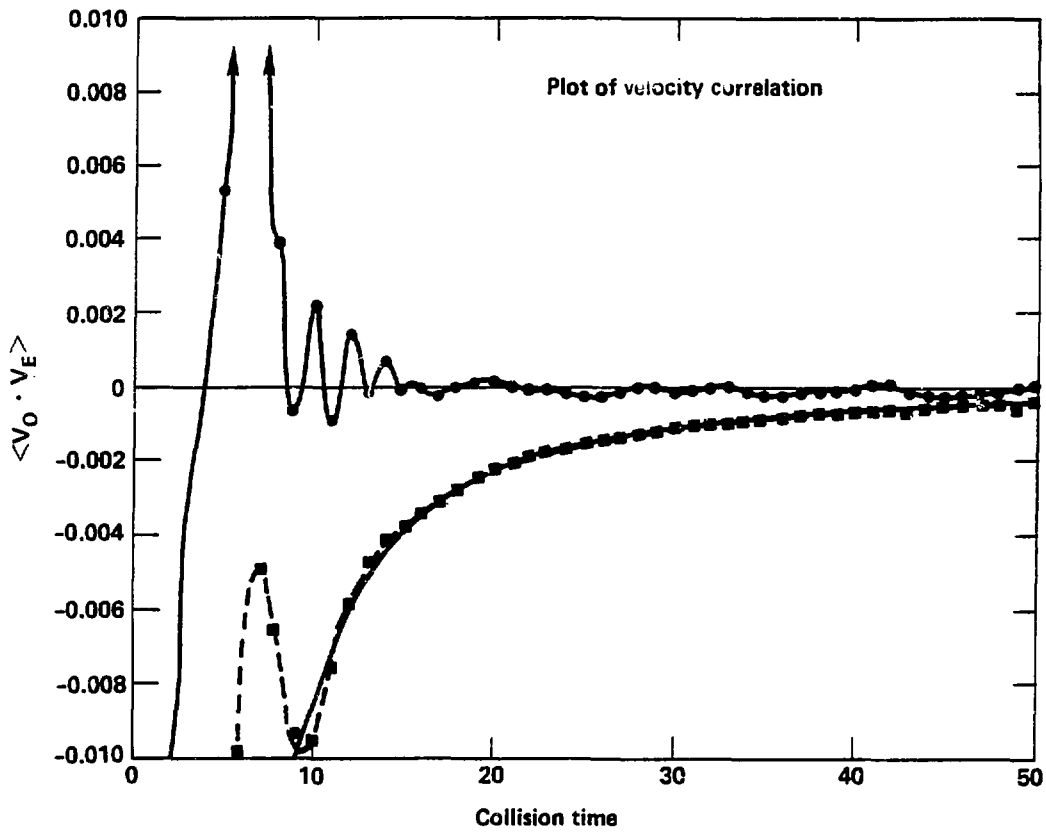


Figure 2

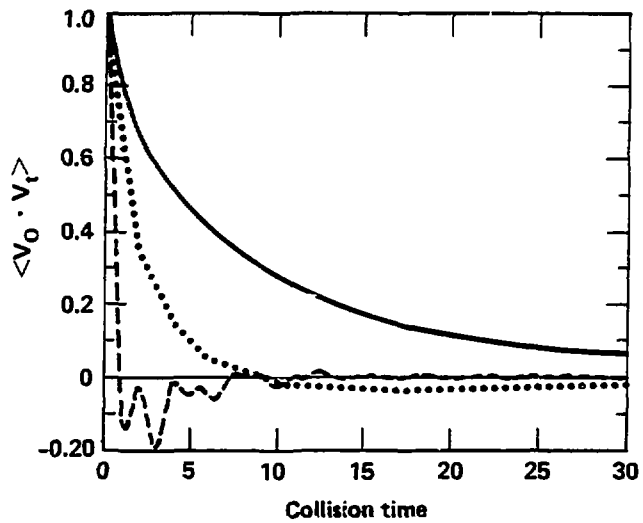


Figure 3

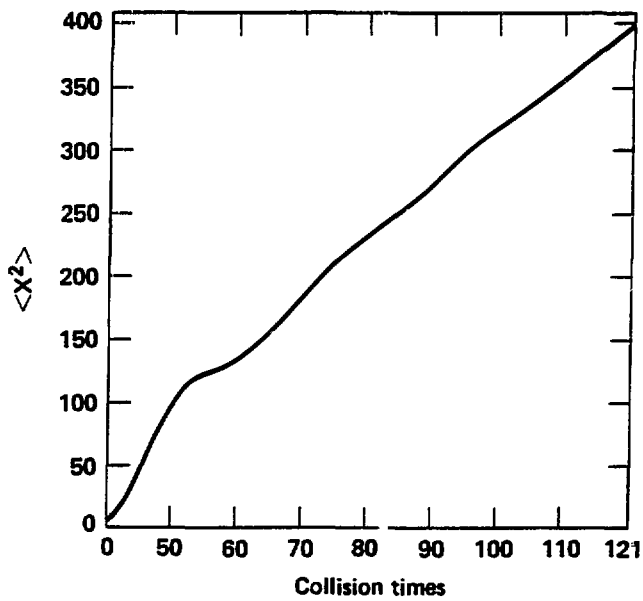


Figure 4

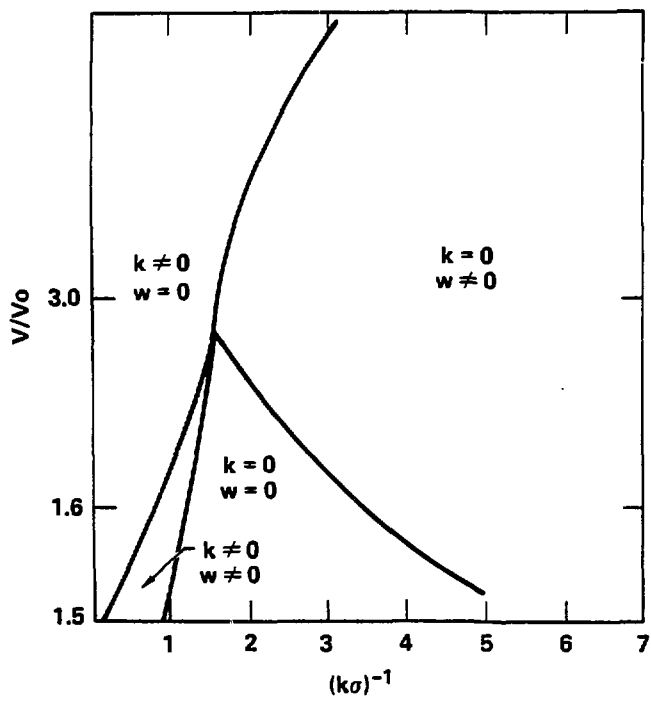


Figure 5